

OPTICAL TRANSMISSION OF INFORMATION

PACS numbers: 42.79.Sz; 42.81.Dp
DOI: 10.1070/QE2015v045n01ABEH015391

Dependence of the bit error rate on the signal power and length of a single-channel coherent single-span communication line (100 Gbit s^{-1}) with polarisation division multiplexing

N.V. Gurkin, V.A. Konyshev, O.E. Nanii, A.G. Novikov, V.N. Treshchikov, R.R. Ubaydullaev

Abstract. **We have studied experimentally and using numerical simulations and a phenomenological analytical model the dependences of the bit error rate (BER) on the signal power and length of a coherent single-span communication line with transponders employing polarisation division multiplexing and four-level phase modulation (100 Gbit s^{-1} DP-QPSK format). In comparing the data of the experiment, numerical simulations and theoretical analysis, we have found two optimal powers: the power at which the BER is minimal and the power at which the fade margin in the line is maximal. We have derived and analysed the dependences of the BER on the optical signal power at the fibre line input and the dependence of the admissible input signal power range for implementation of the communication lines with a length from 30–50 km up to a maximum length of 250 km.**

Keywords: *single-span fibre-optic communication line, differential phase modulation, optical signal-to-noise ratio, coherent detection, electronic chromatic dispersion compensation, nonlinear distortions, nonlinear noise, amplified spontaneous noise.*

1. Introduction

The need in increasing the amount and rate of information transfer conditioned by the increasing computerisation of society, Internet development, growth in the number of mobile network subscribers (including, those using the LTE technology) and popularity of video conferencing, etc. requires a further exponential growth in the bandwidth capability of optical networks and communication systems [1, 2]. To ensure the bandwidth capacity growth, conventional long-range communication systems with amplitude modulation and a channel rate of 10 Gbit s^{-1} are replaced by communication systems with phase modulation and a channel rate of 40 Gbit s^{-1} and by coherent communications systems with a channel rate of 100 Gbit s^{-1} [3–9].

The transition to communications systems with a channel rate of 100 Gbit s^{-1} and coherent detection has dramatically changed the character of nonlinear distortions of optical signals in communication lines [7–14]. In fibre-optic data transmission systems without compensation of periodic dispersion, the optical field becomes random due to dispersive effects that lead to a spatial overlap of a set of transmitted symbols. Due to a high level of accumulated dispersion, nonlinear effects become attenuated, acquire random nature and manifest themselves upon detection in the form of nonlinear noise [11–15]. A number of published experimental studies have confirmed the possibility of using a nonlinear interference noise model to describe nonlinear distortions in long-haul multi-span communication lines [8, 16–19].

The possibility of using the nonlinear interference noise model to describe nonlinear distortions in multi-span coherent communication lines with dispersion compensation and nonlinear distortions in single-span coherent communication lines is not obvious and has been neither theoretically justified nor experimentally investigated.

Thus, the experimental and theoretical research on the behaviour of propagation of optical information signals in single-span coherent communication lines is exceedingly urgent. In this paper, we study experimentally and theoretically the dependences of the BER on the signal power and length of a 100-Gbit s^{-1} single-channel coherent single-span communication line with polarisation division multiplexing. The measured and calculated dependences of the BER are used to find optimal signal powers for the lines of different lengths, at which the BER and the fade margin attain their minimum and maximum, respectively, and to determine the range of admissible input signal powers, i.e., the power range at which the BER value does not exceed the permissible level.

2. Experimental setup

The experimental setup for measuring the optical parameters of a single-span communication line is shown in Fig. 1. The information optical signal at 1558.17 nm (the 24th channel of the standardised ITU-T frequency mesh) passes from an optical transmitter (OT) through an optical multiplexer (MUX) to the input of an erbium-doped fibre amplifier (EDFA1) having a noise factor NF = 6 dB, and, after amplification, enters into a span prototype of a fibre-optic line assembled in the form of two or more sequentially fusion spliced fibre segments 50 km each, reeled on the drums. The prototype uses standard single-mode fibre (SSMF) (ITU-T G.562 standard) with attenuation of 0.2 dB km^{-1}. At the exit of the line prototype, the optical signal is amplified by EDFA2 with a noise factor NF = 6 dB, and after passing through a tunable fibre attenuator (TFA1), two couplers (C) and a demultiplexer (DEMUX), enters into an optical receiver (OR).

N.V. Gurkin, V.A. Konyshev, A.G. Novikov, V.N. Treshchikov, R.R. Ubaydullaev T8 LLC, Krasnobogatyrskaya ul. 44/1, office 826, 107076 Moscow, Russia; e-mail: rru@t8.ru, novikov@t8.ru;
O.E. Nanii Department of Physics, M.V. Lomonosov Moscow State University, Vorob'evy Gory, 119991 Moscow, Russia; T8 LLC, Krasnobogatyrskaya ul. 44/1, office 826, 107076 Moscow, Russia; e-mail: naniy@t8.ru

Received 27 January 2014; revision received 21 April 2014
Kvantovaya Elektronika **45** (1) 69–74 (2015)
Translated by M.A. Monastyrskiy

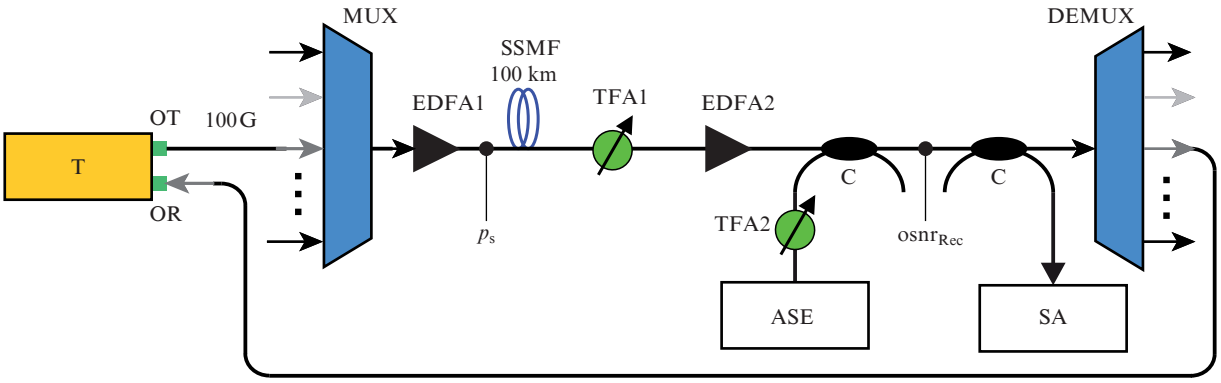

Figure 1. Scheme of the experimental setup: (T) transponder, 100 Gbit s^{-1} (in-built BER-tester); (OT) optical transmitter; (EDFA) erbium-doped fibre amplifier; (SSMF) standard single-mode fibre; (TFA) tunable fibre attenuator; (MUX) multiplexer; (DEMUX) demultiplexer; (ASE) source of amplified spontaneous emission; (SA) spectrum analyser; (C) coupler; (OR) optical receiver.

The transmitter is connected to a source of random signal and its encoding device. The encoding device adds about 15% of forward error correction (FEC).

The receiver incorporates a real-time decoding device that ensures the error correction and counts the number of corrected erroneous BER bits (before FEC). An efficient algorithm for error correction is used to reduce the number of errors from the critical value 1.94×10^{-2} (before FEC) to 1.0×10^{-9} (after FEC), which is required for the qualitative operation of the communication line. In reducing the number of errors prior to FEC, the number of errors after FEC decreases very rapidly (Table 1).

Table 1. BER before and after the FEC and osnr values.*

BER before FEC	BER after FEC	osnr/dB
1.95×10^{-2}	3.2×10^{-9} (errors in the line)	12.24
1.94×10^{-2}	1.0×10^{-9} (critical value)	12.25
1.90×10^{-2}	1.0×10^{-11}	12.29
1.85×10^{-2}	3.2×10^{-14}	12.32
1.80×10^{-2}	$<1.0\times10^{-15}$ (not recorded)	12.37
1.70×10^{-2}	–	12.45
1.0×10^{-2}	–	13.17
1.0×10^{-3}	–	15.46
1.0×10^{-4}	–	17.32
1.0×10^{-5}	–	18.61

* The data were obtained from the 100 Gbit s^{-1} transponder measurements used in the experiment.

The device intended for the analysis of the received signal automatically counts the number of the erroneous bits corrected by the decoder and determines the BER arising in the signal transmission through the communication line under testing.

Two couplers located between the attenuator TFA1 and demultiplexer DEMUX are used to connect the source of amplified spontaneous emission (ASE) and optical spectrum analyser (SA). The attenuator TFA2 is used to adjust the power of the additional noise generated by the ASE source.

Part of experimental measurements was carried out using 100-, 150- and 200-km-long SSMF-based communication line prototypes. It was established that the dependences of the BER on the signal power for the line lengths of 150 and 200 km coincide with similar dependences for the line length of 100 km with additional attenuation of 10 and 20 dB, respectively, generated by the attenuator TFA1. The measured values of the optical signal-to-noise ratio (SNR) at a signal power of 8 dBm are 40, 30 and 20 dB for 100-, 150- and 200-km-long communication lines, respectively. With the same signal power in the 100-km-long line having an attenuation of 0, 10 and 20 dB provided by the attenuator TFA1, the same values of the optical SNR, i.e., 40, 30 and 20 dB, have been obtained. In addition, the 100-km-long line has experimentally demonstrated the equivalence of the two methods of varying the optical SNR at a fixed signal power: by means of the attenuator and with the ASE source.

The first method involves the creation of additional attenuation by means of the attenuator TFA1. In this case, the optical SNR at the receiver is determined by the expression:

$$\begin{aligned}\text{osnr}_{Res} &= -10\lg(h\nu B/1\text{ mW}) + p_s - \alpha L - a_{VOA1} - \text{NF}_{EDFA2}\\ &= 58 + p_s - \alpha L - a_{VOA1} - \text{NF}_{EDFA2},\end{aligned} \quad (1)$$

where h is the Planck constant; $\nu = 193.1\times10^{12}$ Hz is the carrier frequency; $B = 12.5\times10^{9}$ Hz is the reference optical band [hence, $10\lg(h\nu B/1\text{ mW}) = -58$]; p_s (dBm) is the signal power at the SSMF span input; α (dB km^{-1}) is the signal attenuation at 1 km; and L (km) is the fibre length.

The values of the optical SNR are given hereafter relative to the reference bandwidth 12.5 GHz (~0.1 nm).*

The second method is associated with the introduction of additional noise from the ASE source. In this case, there is no attenuator ($a_{VOA1} = 0$), and the optical SNR at the receiver appears as

$$\text{osnr}_{Rec} = 58 + p_s - \alpha L - 10\lg\left(F_{EDFA2} + \frac{F_{ASE} - 1}{G_{EDFA2}}\right), \quad (2)$$

*To designate the system parameters that characterise the ratios of some values expressed in linear units, we use the capital letters [attenuation A, optical signal-to-noise ratio OSNR, gain G, and power P (in mW)]. For the same parameters expressed in dB (power – in dBm) the lower case letters (a, osnr, g and p) are used, respectively).

where $F_{EDFA2} = 10^{0.1NF_{EDFA2}}$ is the noise factor of TFA2; $F_{ASE} = A_{sp}[1 + P_{ASE}/(h\nu\Delta\nu)]$ is the effective noise factor of the element that introduces noise; A_{sp} are the losses on the coupler; and P_{ASE} is the power of a noise introduced at the point after the attenuator.

The equivalence of the two methods of measurement means that, at equal values of $osnr_{Rec}$ and p_s, the measured values of the BER for different ways of reducing the optical SNR turn out equal. The equivalence of the methods of introducing additional noise and additional attenuation opens the possibility of measuring the fade margin by means of the first method.

Information is transmitted with the use of four-level phase modulation and polarisation division multiplexing (DP-QPSK modulation format) [5]. At a 100-Gbit s^{-1} transmission rate of useful information and 20% of redundant information (15% takes encoding for error correction, 5% – headers and other service information), the total information rate is 120 Gbit s^{-1}. At a symbol efficiency of 4 bits per symbol, the symbol stream rate constitutes 3×10^{10} symbol s^{-1}.

The multiplexer MUX in this scheme operates as a narrow-band optical filter with a bandwidth of 30 GHz.

To calibrate the transponder, we measured the BER as a function of $osnr_{Rec}$ (Fig. 2). The measuring scheme coincides with that shown in Fig. 1, the line prototype being replaced by a short fibre span of several meters long.

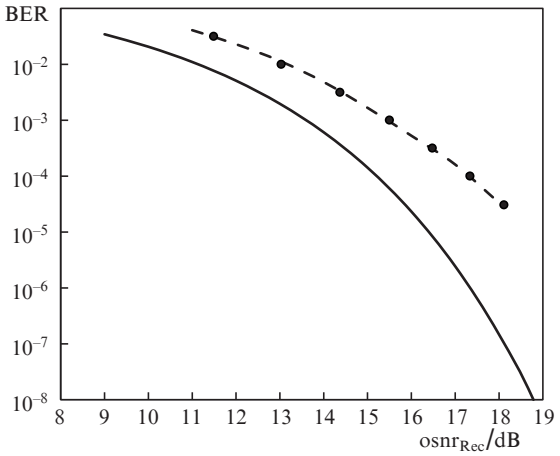

Figure 2. Dependence of the BER before FEC on $osnr_{Rec}$ for a 100-km-long line. Solid curve represents a theoretical limit according to formulas (5) and (6), points show the experiment (transponder calibration), the dashed line – modelling.

3. Dependence of the BER on the signal power in a 100-km-long line (experiment and phenomenological formula)

The BER is a key parameter that determines the quality of a fibre-optic communication line, since its increase with increasing communication line length represents the main factor restricting the range of line operation.

Experimental dependences of the BER on the signal power are shown in Fig. 3. It is seen that in the linear regime (at low input signal powers) the BER decreases with increasing p_s. However, after that, with increasing signal power, the nonlinear effects begin to appear, which originally cause slowing of the BER decrease with increasing p_s, and then even result in the BER increase. Thus, at a certain signal power (P_B), the BER reaches its minimum. At a fixed level of nonlinear distortions, the P_B value increases with the ASE noise level. This means that the effect of nonlinear signal degradation is less noticeable against the background of the high noise level.

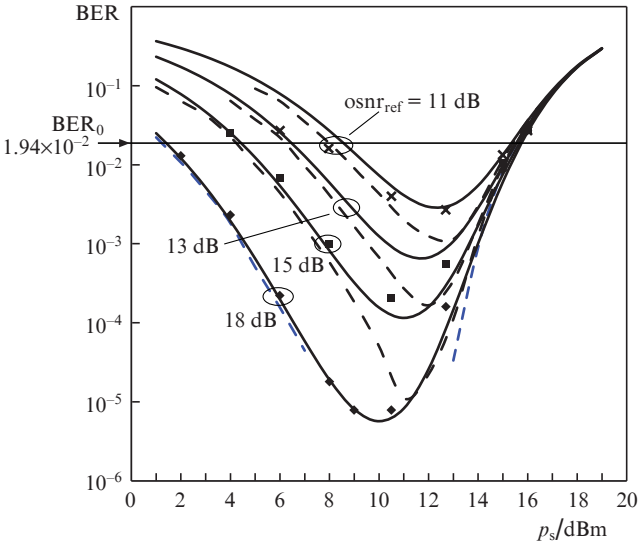

Figure 3. Dependence of the BER before FEC on p_s at $osnr_{ref}$ = (×) 11, (■) 13, (■) 15 and (♦) 18 dB ($osnr_{ref} = osnr_{ASE}$ at p_s = 8 dBm). Marked is the critical level of the bit error rate BER_0. For all $osnr_{ref}$: points show the experiment, solid curves – theoretical calculation, dashed lines – numerical modelling.

To explain the experimental dependences, let us assume that even in the case of a short line (~100 km), the manifestation of nonlinear effects can be described as the occurrence of nonlinear noise produced in fibre. We also assume that, similar to long lines [15], the nonlinear noise P_{NL} represents an addition to the ASE noise P_{ASE}:

$$P_\Sigma = P_{NL} + P_{ASE}. \tag{3}$$

As shown in [8], in measuring the optical SNR with an optical spectrum analyser, the value $OSNR_{ASE} = P_s/P_{ASE}$ is in fact measured. Following work [8, 15], let us introduce the concept of a total optical SNR:

$$OSNR_\Sigma = P_s/P_\Sigma. \tag{4}$$

The thus defined $OSNR_\Sigma$ value is fundamentally related with the BER and the parameter Q:

$$BER = \frac{1}{2}\mathrm{erfc}\left(\frac{Q}{\sqrt{2}}\right), \tag{5}$$

$$Q = \sqrt{\frac{B_O}{B_E}OSNR_\Sigma}, \tag{6}$$

where B_O/B_E is the ratio of the optical and electrical bandwidths. The parameter Q, which is often called the Q-factor, characterises the signal quality. In particular, this parameter is associated with the eye-diagram aperture and by its value is close to the SNR at the point of the maximum of the eye-diagram aperture.

We introduce the parameter OSNR_Σ analogous to the classical parameter OSNR_{NL}:

$$\mathrm{OSNR}_{NL} = P_s/P_{NL}. \quad (7)$$

From the additivity of the linear and nonlinear noise, we obtain the relation

$$\mathrm{OSNR}_{ASE}^{-1} + \mathrm{OSNR}_{NL}^{-1} = \mathrm{OSNR}_\Sigma^{-1}. \quad (8)$$

The nonlinear noise power P_{NL} can be determined by formula (9), which is valid for long lines [8] (the validity of this formula for short single-span lines is not obvious and is experimentally confirmed in the present work):

$$P_{NL} = \eta P_s^3/A, \quad (9)$$

where P_s (in mW) is the useful signal power at the input into the homogeneous fibre span; A are the losses in this span in linear units; and η (in mW^{-2}) is the nonlinear noise constant representing a characteristic parameter of fibre. The equivalent nonlinear noise power referred to the fibre span input is $P_{NL} = \eta P_s^3$. As shown by experimental studies, the equivalent nonlinear noise power in a short-span line ($L \ll 1/\alpha$), when attenuation can be neglected, increases in proportion to the fibre length. However, in a long-span line ($L \gg 1/\alpha$), the nonlinear noise constant η does not depend on the span length and total losses in the span. This allows us to describe the dependence of η on the losses in fibre as

$$\eta = \frac{L_{eff}(L)}{L_{eff}(\infty)}\eta_0, \quad (10)$$

where $L_{eff}(L) = [1 - \exp(-\alpha_0 L)]\alpha_0^{-1}$; α_0 (in km^{-1}) $\approx 0.23\alpha$; and η_0 is the nonlinearity constant at $L \gg 1/\alpha$.

Thus, for a single-span line we obtain a simple formula relating the total SNR with the input signal power:

$$\frac{1}{\mathrm{OSNR}_\Sigma} = \frac{AF h\nu \Delta\nu}{P_s} + \eta P_s^2. \quad (11)$$

The BER value can be easy calculated by using (5), (6) and (11). The results of BER calculation as a function of the power p_s for different line lengths (or at different noise levels) are shown in Fig. 3. Note that only one adjustable parameter, the nonlinear noise constant η, has been used in the calculations.

As can be seen from Fig. 3, the simple phenomenological formula describes quite well the experimental results. This allows one to use this formula for optimising the communication lines and evaluating the system parameters. It also explains the behaviour of the dependences of the BER on the input signal power. Because the total noise power is determined by the contribution of the P_{ASE} component independent of the signal power and by the contribution of the P_{NL} component proportional to P_s^3, the OSNR_Σ value (11) attains its maximum at a certain signal power:

$$P_B = \left(\frac{AF h\nu \Delta\nu}{2\eta}\right)^{1/3}. \quad (12)$$

As follows from (12), an increase in the noise power P_{ASE} leads to an increase in the signal power corresponding to the minimal BER.

4. Numerical simulation using OptSim

Let us compare the results of experimental studies with the results of numerical simulations that have been performed using the OptSim software package. We used this package in the Sample mode. The modelling circuit structure is shown in Fig. 4.

In the numerical model, we used a standard scheme of the optical transceiver [8]. The optical signal is emitted in two polarisations by means of the optical transmitter (OT) based on the Mach–Zehnder modulator. A super-Gaussian second-order filter describes the multiplexer behaviour. The amplifier EDFA1 sets the power to be launched into fibre. The Manakov equations [20] that take into account two polarisations of the optical signal in fibre are used to model the optical signal propagation in SSMF fibre. Thus, numerical modelling can be used to calculate the actual communication lines. The attenuator TFA1 allows the optical circuit parameters to be varied without the risk of going beyond the limits of admissible values. The amplifier EDFA2 provides a constant input power to the receiver transponder. The input power is stabilised at the level of 0 dBm. The DEMUX filter describes the demultiplexer behaviour and has the parameters similar to the multiplexer. The circuit element located behind the demultiplexer simulates the transponder receiver (TR) with the function of BER measurements.

In modelling a standard optical fibre, the following parameters have been used: $L = 100$ km, $\alpha = 0.2$ dB km^{-1}, $D = 16.5$ ps nm^{-1} km^{-1}, $n_2 = 3.33\times10^{-20}$ m^2 W^{-1}, and $A_{eff} = 80$ $\mu\mathrm{m}^2$. We should note that these simulation parameters are in good agreement with the experimental data.

The dependences of the BER on the DP-QPSK signal power (120 Gbit s^{-1}), measured numerically for a 100-km-long single-span fibre line at different values of additional noise (line length), are shown by dashed curves in Fig. 3.

As a result of numerical simulation, the empirical nonlinearity parameter η_0 was determined, which was found to be

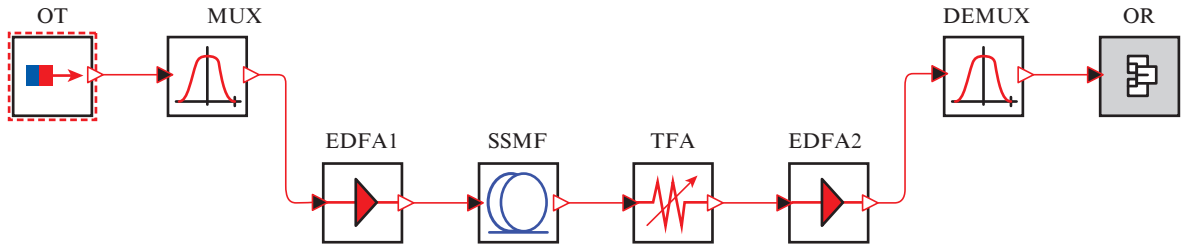

Figure 4. Modelling scheme for determining OSNR_{Res}.

$(4.0 \pm 0.3) \times 10^{-5}$ mW^{-2} for the optical fibre in question. The comparison with experimental data have shown that the numerical results well describe the real experiment at the BER values up to FEC from 1×10^{-3} to 3×10^{-2}.

5. Dependence of optimal powers and admissible power range of the input signal on the communication line length

If the span length is less than the maximum admissible one, information can be transmitted in a certain signal power range that depends on the line length (Fig. 5). The area between the upper and lower curves determines the range of admissible input powers at which the communication line is operational. Theoretical dependences of the maximum and minimum admissible input powers on the line length in Fig. 5 are obtained from formulas (16) and (17) (given below), whilst the values of these powers with regard to the criterion BER = 10^{-9} are obtained after the error correction. Points on the graphs show the results of the numerical simulation.

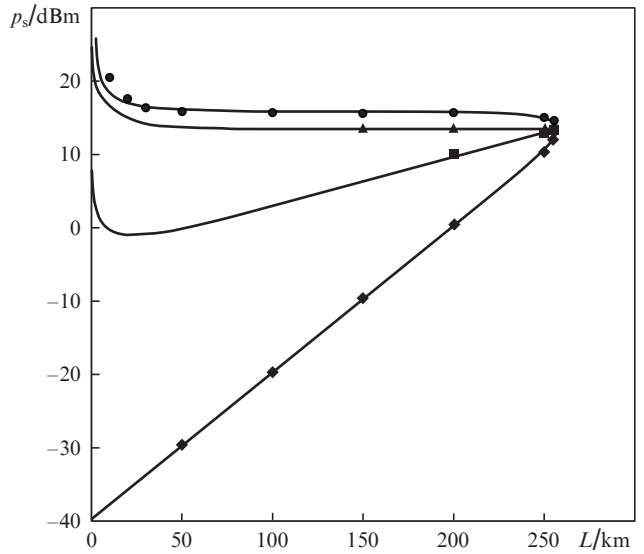

Figure 5. Dependences of optimal powers and admissible input signal power range p_s^{max} (●) – p_s^{min} (♦) as well as $OSNR_M^{max}$ (▲) and BER^{min} (■) on the line length. Solid curves show theoretical calculation, points – numerical modelling.

The upper limit of the range of admissible input signal powers is constant over a wide range of span lengths and is equal to 16 dBm, herewith the optimal value of the input power being p_M = 13.5 dBm (p_M is the input signal power at which the ratio $OSNR_M = OSNR_{NL}/OSNR_{Rec}$ attains its maximum, the so-called OSNR margin).

The lower limit of the range of admissible input signal powers is determined by the ASE noise, which increases with increasing span length. Because the nonlinear noise level throughout the region of span lengths, except the maximal lengths (i.e. up to about 250 km) is negligibly small, the minimum admissible signal power p_s increases linearly with the span length. In other words, at signal powers typical of the lower limit of the admissible power range, the required OSNR value of the line virtually coincides with the OSNR value in the 'back-to-back' scheme, since nonlinear distortions are negligible in this case. A linear increase in the minimal admissible power is conditioned by an increase in the noise level with increasing span length. However, for $L > 250$ km, a noticeable contribution of the nonlinear distortions appears even at the lower limit of admissible powers.

The upper limit of admissible p_s values is determined by the level of nonlinear signal distortions. In this area, the communication system operates in a strongly nonlinear regime. Because the nonlinear noise power at $L > 30$ km does not depend on the fibre length, the maximum admissible power p_s^{max} is virtually constant up to the length of $L \approx 200$ km when the ASE noise influence can be neglected. In this region, at a signal power of 16 dBm, the equivalent nonlinear noise power p_M reduced to the 0.1-nm band should be equal to the critical noise value p_{ASE}^{max}, where

$$p_{ASE}^{max} = p_s - \mathrm{osnr}_{btb}. \tag{13}$$

The experimentally measured value of p_{ASE}^{max} constituted 3.7 dBm.

As is seen from Fig. 5, the optimal power values obtained, on the one hand, in accordance with the criterion of maximising the $OSNR_M$ and, on the other, at reaching the minimum BER^{min}, do not coincide – the first value is always greater than the second one. To explain this discrepancy, one should refer to the dependences of the BER on the power at different line lengths, i.e., at different ASE noise levels (see Fig. 3). With increasing ASE noise power, the signal power providing the lowest error level increases. The optimal power ensuring the greatest OSNR margin corresponds to the power providing BER^{min} at the maximum power of the ASE noise (or at the maximum length of the communication line). This means that the power that provides the largest margin for the OSNR exceeds the power that minimises the BER performance in the entire region of the communication line operation, and only at the maximum line length these power values coincide (see Fig. 5)

In work [8], an explicit analytical expression for the power P_M that corresponds to the $OSNR_M^{max}$ maximum is obtained

$$P_M = (3\eta \mathrm{OSNR}_{btb})^{-1/2}. \tag{14}$$

The maximal fade margin of the line at $P_s = P_M$ ensures maximal reliability of the communication line operation. We consider the maximal reliability as the line operation regime when the line remains workable at the maximum level of additional losses that may result from the fibre cable damage or degradation.

The admissible power range boundaries P^{min} and P^{max} can be found from the analytical expressions:

$$\varphi = \frac{1}{3}\arccos((P_B/P_M)^3), \tag{15}$$

$$P^{min} = 2P_M \cos\left(\frac{1}{3}\pi + \varphi\right), \tag{16}$$

$$P^{max} = 2P_M \cos\left(\frac{1}{3}\pi - \varphi\right). \tag{17}$$

As can be seen from Fig. 5, for the typical line lengths of 30–50 km, the range of admissible input signal powers is broad and varies from –30 to about 15 dBm. The maximum length of a single-span line may amount to 250 km, but only in the case of an optimal power of about 15 dBm. If the line length is close to its maximum, the admissible input power range rapidly tends to zero.

6. Conclusions

A simple phenomenological formula (11), as it follows from Fig. 3, provides an accurate description of experimental dependences of the BER on the signal power and length of the coherent single-span communication line.

It has been established that the range of admissible input signal powers, i.e., the powers at which the BER after FEC does not exceed the critical value of 10^{-9}, is decreased in such a way that an increase in the line length keeps its upper boundary constant, whilst its lower boundary increases.

It has been experimentally and theoretically shown that, in SSMF-based communication lines with the length exceeding 50 km, the signal power at which the maximum OSNR margin is attained does not virtually change if the single-span line length varies. The signal power, at which the BER minimum is achieved, increases with the single-span line length (for a length of more than 30 km).

References

1. Winzer P.J. *Proc. ECOC* (London, 2013) Paper We.1.D1.
2. Tkach R.W. *Bell Labs Tech. J.*, **14** (4), 3 (2010).
3. Redyuk A.A., Shtyrina O.V., Nanii O.E., Kapin Yu.A., Sachalin E.A., Titov E.B., Treshchikov V.N., Yaryshkin A.A., Fedoruk M.P. *Kvantovaya Elektron.*, **41** (10), 929 (2011) [*Quantum Electron.*, **41** (10), 929 (2011)].
4. Gurkin N.V., Kapin Yu.A., Nanii O.E., Novikov A.G., Pavlov V.N., Plaksin S.O., Plotskii A.Yu., Treshchikov V.N. *Kvantovaya Elektron.*, **43** (6), 546 (2013) [*Quantum Electron.*, **43** (6), 546 (2013)].
5. Nanii O.E., Treshchikov V.N. *Vestnik Svyazi*, **4**, 52 (2011).
6. Nanii O.E., Novikov A.G., Plotskii A.Yu., Treshchikov V.N., Ubaidullaev R.R. *Elektrosvyaz'*, **6**, 40 (2012).
7. Gurkin N.V., Nanii O.E., Treshchikov V.N., Ubaidullaev R.R. *Vestnik Svyazi*, **1**, 39; **2**, 40 (2013).
8. Gurkin N.V., Nanii O.E., Novikov A.G., Plaksin S.O., Treshchikov V.N., Ubaidullaev R.R. *Kvantovaya Elektron.*, **43** (6), 550 (2013) [*Quantum Electron.*, **43** (6), 550 (2013)].
9. Gainov V.V., Gurkin N.V., Lukinih S.N., Akopov S.G., Makovejs S., Ten S.Y., Nanii O.E., Treshchikov V.N. *Laser Phys. Lett.*, **10**, 075107 (2013).
10. Gainov V.V., Gurkin N.V., Lukinih S.N., Nanii O.E., Treshchikov V.N. *Proc. ICONO/LAT* (Moscow, 2013) Paper LWD2.
11. Poggiolini P., Carena A., Curri V., Bosco G. *IEEE Photon. Technol. Lett.*, **14**, 742 (2011).
12. Carena A., Curri V., Bosco G., Poggiolini P. *J. Lightwave Technol.*, **30** (10), 1524 (2012).
13. Carena A., Bosco G., Curri V., Poggiolini P., Taiba M.T., Forghieri F. *Proc. ECOC* (Torino, Italy, 2010) Paper P4.07.
14. Sinkin O.V., Cai J.-X., Foursa D., Zhang H., Pilipetskii A., Mohs G., Bergano N. *Proc. OFC/NFOEC* (Los Angeles, CA, USA, 2012) Paper OTu1A.2.
15. Poggiolini P. *J. Lightwave Technol.*, **30** (24), 3857 (2012).
16. Torrengo E., Cigliutti R., Bosco G., Carena A., Curri V., Poggiolini P., Nespola A., Zeolla D., Forghieri F. *Proc. ECOC* (Geneva, Switzerland, 2011) Paper We.7.B.2.
17. Vacondio F., Simonneau C., Lorcy L., Antona J.-C., Bononi A., Bigo S. *Proc. ECOC* (Geneva, Switzerland, 2011) Paper We.7.B.1.
18. Nanii O.E. *Vseros. konf. po volokonnoi optike* (Proc. All-Russian Conf. on Fibre Optics) (Perm, 2013) A10-1.
19. Gurkin N.V., Nanii O.E., Novikov A.G., Plaksin S.O., Treshchikov V.N., Ubaydullaev R.R. *Proc. ICONO/LAT* (Moscow, 2013) Paper LWD4.
20. Agrawal G. *Nonlinear Fiber Optics* (San Diego: Acad. Press, 1995; Moscow: Mir, 1998).